IJCSE International Journal of Computer Sciences and Engineering Open Access
Research Paper Vol.-7, Issue-6, June 2019 E-ISSN: 2347-2693

Coded Phase Gradient Metasurface Antenna Design for X- Band Radar

Monalisa Nayak[1*], Devika Jena[2], Kodanda Dhar Sa[3], Dillip Dash[4]

[1,2,3] Department of Electronics and Tele Communication, Indira Gandhi Institute of Technology, Odisha, India
[4]School of Electronics Engineering, VIT University, Vellore, India

Corresponding author:dillipdash106@gmail.com

DOI: https://doi.org/10.26438/ijcse/v7i6.695703 | Available online at: www.ijcseonline.org

Accepted: 12/Jun/2019, Published: 30/Jun/2019

***Abstract*—** To achieve long distance coverage and better resolution, high gain antennas is convenient for airborne radars. So a great deal of attention has been devoted to exploiting new approaches towards the problem. Radar application demands a low profile, minimal weight and high gain antennas. Over the last decade microstrip antennas are used as an alternative element for the bulky and heavy weight reflector antennas. Presently researchers are implementing metasurface antennas and their imitative for the radar applications. A high gain transmitting microstrip lens antenna is presented by putting a layered phase gradient coded metasurface with 0 & 1 elements for 0 and π phase responses. Four types of unit cell with two bits coding elements 00,01,10,11 is implemented for four phase differences. The lens antenna results a gain enhancement of 11.7 dbi and return loss of -34 dB, which is approximately 7 dbi and -17dB in case of a normal microstrip antenna, so the gain is enhanced by 4.7dB and a return loss is reduced by 17 dB at 10.3 MHz frequency.

***Keywords*—**Codded phase gradient, Lens, Metasurface, Microstrip, X-Band Radar.

I. INTRODUCTION

Presently the radar antenna design system focuses on developing of low cost with minimal weight, high gain and low profile antennas having capability to maintain high performance over a wide range of frequencies [1]. To exploit waveform diversity and achieve degrees of freedom multiple input multiple output (MIMO) radars are currently used for deference applications. This requires the development of low profile antenna arrays to achieve spatial resolution and spatial diversity in addition to range and Doppler resolution [2]. As a solution to the design constraint generally five approaches are put forward names as antenna arrays, reflectors, cavities and lens antennas [3, 4]. To attain high gain and low side lobes conventional antenna array system requires a complex feeder network and more power distribution. However, reflectors like parabolic reflectors have large profile and hard fabrication process [5, 6]. The cavities where the substrates made thinner, are compatible and low cost but are confined to narrow bandwidth and high side lobes. Numerous researchers incorporating lens antennas to enhance the gain, but it requires hard fabrication and suffers from signal loss to some extent [7, 8]. To overcome the limitations of the classical antenna array, a high gain lens antenna is designed at X-band frequency by considering the generalized Snell's law using super cells for optimized and high transmission efficiency [9]. Metasurface belongs to the class of lens antennas. The design of metasurface has been receiving tremendous attention in the last years and currently one of the major components in designing radar antennas that are used as an alternative to the bulky and heavy weight reflection array antennas. A metasurface is a two dimensional metamaterial made up of a single layer of microscopic unit cell, i.e. an artificial thin film whose width is much smaller than the operating wavelength, which is projected to exhibit specific macroscopic properties [10, 11]. Yu et al. proposed the phase gradient metasurface (PGMS) a special kind of metasurface which has been demonstrated using the generalization of the Snell's law to manipulate the direction of reflecting and refracting waves [12]. H. Li et al. [1] presented a high gain transmitting lens antenna using PGMS where the patch antenna is located at the focal point of the MS as a feed source, and the quasi-spherical wave emitted by the source is transformed to plane wave, by which the beam width of the antenna decreased and gain has been enhanced. K. S. Beenamole [8] presented the linear dependency between the dielectric thickness and bandwidth [13, 14]. It can be observed that for a specified permittivity of the substrate, the radiation resistance and efficiency of the antenna decreases, but as the substrate thickness increases the radiation pattern and gain increases.

In this communication a high gain transmitting microstrip lens antenna with layered phase gradient and digitally coded metasurface is proposed for the X-band radar applications.

Here the generalized Snell's law of anomalous reflection using super cell is described by introducing abrupt changes of phase on the ultrathin metasurace. The digital metasurface uses the 0 and 1 element for the 0 and π phase response. It is observed that the metasurface results a gain enhancement of 11.7 dbi, which is approximately 7 dbi in case of normal microstrip antenna. And also the lens antenna gives a power delay or return loss about -17 db. The performance of S_{11} parameter between a normal microstrip antenna and coded metasurface antenna is compared in terms of power delay and return loss.

II. DESIGN OF META ATOMS

Meta atoms or the unitcell consists of four metallic layers with three intermediate dielectric layers. Inside the metallic layer a solid circle patch and a square ring in outside of the circle are present. By using the concept of the periodic boundary unit cell is simulated in the CST 2016 microwave software, where the permittivity of dielectric layers and thickness are 2.65 and 1.5mm respectively.

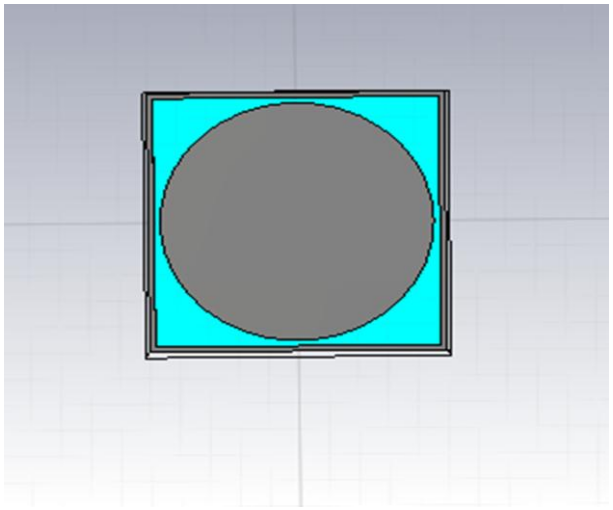

Figure 1. Structure of the front view of simulated setup of the phase gradient metasurface element with four metallic layer.

The structure of the front view and perspective view of the phase gradient metasurface element composed of four metallic layers and three dielectric layers which are shown in Fig. 1 and Fig. 2 respectively.

The phase gradient can be controlled by varying the radius of the unit circle, i.e. $r_n \leq 4.6$ mm by keeping d=1.5mm, p=10mm and t=0.02mm constant. It is observed that for a three layered unit cell the amplitude of the transmission coefficient at 10 GHz is greater than 0.8 when the radius of the solid circle is less than 4.6 mm. and the phase comes in the range between $[0, 360]$ which satisfies the requirements for the PGMS antenna design.

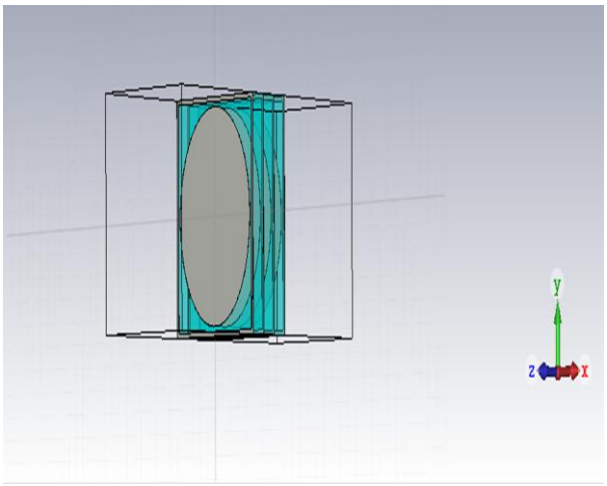

Figure 2. Structure of the perspective view of simulated setup of the phase gradient meta surface element with four metallic layer**.**

A. Validation of AnomalousReflection

To validate the design of the phase gradient metasurface elements that results high efficiency with anomalous refraction having a phase range span of [0,360], a supercell with linear phase gradient is designed. The supercell consists of eight elements are arranged horizontally whose transmission phase and amplitude at 10 GHz. The discrete phase shift supercells are designed in steps of 45^0 and its amplitude of the transmission coefficient is greater than 0.85 at $r_o \leq 4.6$. Phase and amplitudes of the S_{21}values for single, double and three layer dielectrics are designed with $r_1 = 1.15$ mm, $r_2 = 2.88$ mm, and $r_3 = 4.6$ mm and shown in Fig. 3 & 4. It can be observed from the figure that as the number of dielectric layers increases in the unit cell the phase range increases.

According to the generalized law of reflection given in (1), the reflected wave will always deflect in a phase delay direction [9]

$$\sin(\theta_r) - \sin(\theta_i) = \lambda/2\mu\, n_i \left(\sqrt{(d\varphi/dx)^2 + (d\varphi/dy)^2}\right) \quad (1)$$

Where φ is the phase discontinuity, n_i is the refractive index of the incident medium, θ_r and θ_i denotes the reflected wave and incident wave of the electromagnetic wave respectively, λ is the wavelength, $d\varphi/dx$ and $d\varphi/dy$ represents the phase gradient along x and y directions respectively.
By substituting $d\varphi/dx = d\varphi/dy$, equation (1) becomes

$$\sin(\theta_r) - \sin(\theta_i) = \sqrt{2}\lambda/2\pi\, n_i\ (d\varphi/dy) \quad (2)$$

The phase shift across a single unitcell is $\Delta\varphi = 2\pi/n$, n is the number of unitcells. The phase gradient is calculated as $2\pi/n\, p$. Under normal incidence θ_r is calculated as

$$\theta_r = sin^{-1}\left(\sqrt{2}\lambda/np\right) \quad (3)$$

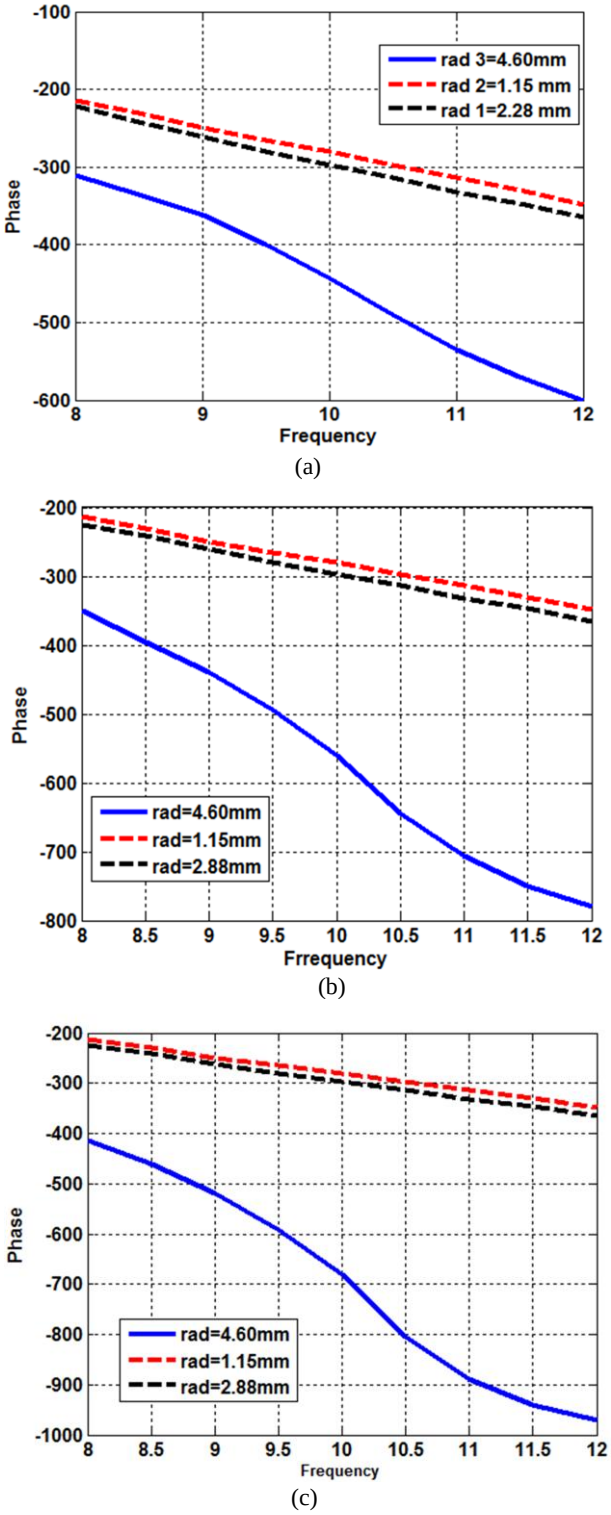

Figure 3. (a) Phase of single layered dielectric (b) phase of double layered dielectric (c) phase of three layered dielectric

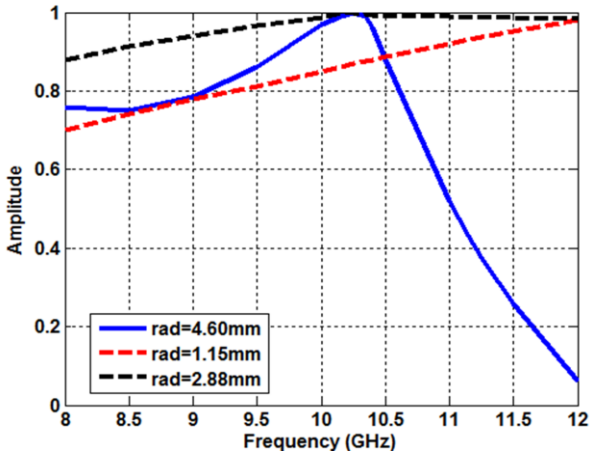

Figure 4. Amplitude values of S21 parameter for different radius ranges of three layered dielectric.

In the design, the sample is placed in free space where the refractive index is unity. Thus θ_t can be obtained as (4).

$$\theta_t = sin^{-1}(\lambda/2\pi * 2\pi/np) \quad (4)$$

As the supercell is composed of 8 elements with $r_o \leq 4.6$, that are $r_1 = 2.16$ mm, $r_2 = 2.97$ mm, $r_3 = 3.65$ mm, $r_4 = 3.78$ mm, $r_5 = 4.22$ mm, $r_6 = 4.42$ mm, $r_7 = 4.52$ mm and $r_8 = 4.60$ mm. Figure 4 shows the simulated transmission phase and amplitude of the eight supercells at 10 GHz frequency.

To enhance the gain of the antenna the unitcell is used when the plane are focused through a phase gradient meta surface in the orthogonal plane and it is observed that by selecting the focal distance 30 mm better consistency can be achieved. In this work four radius elements are used as $r_1 = 2.16$ mm, $r_2 = 2.97$ mm, $r_3 = 3.78$ and $r_4 = 4.60$ mm. The phase and amplitude of S_{21} and S_{11} parameters for three dielectric layers are shown in Fig 5.

It has been observed that for the three dielectric layer the magnitude of the S_{21} parameter decreases as the frequency increases from 10.6 GHz for the $r_o = 4.60$ mm and for other radii the magnitude values are almost in the range of 0 to -2 dB. In case of phase of the S_{21} parameter for the $r_o = 4.60$ mm the phase is nearly120^0. Figure 5 shows the magnitude and phase response of the S_{11} parameter of three dielectric layer.

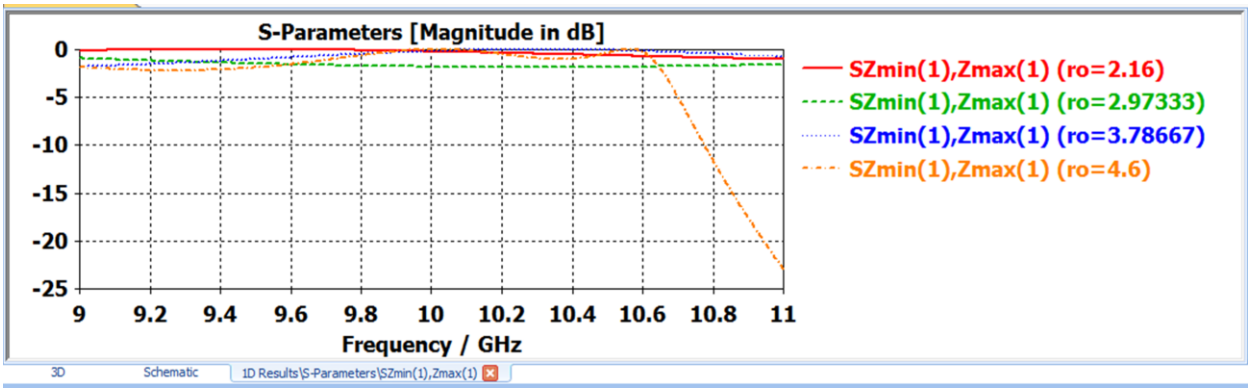

(a)

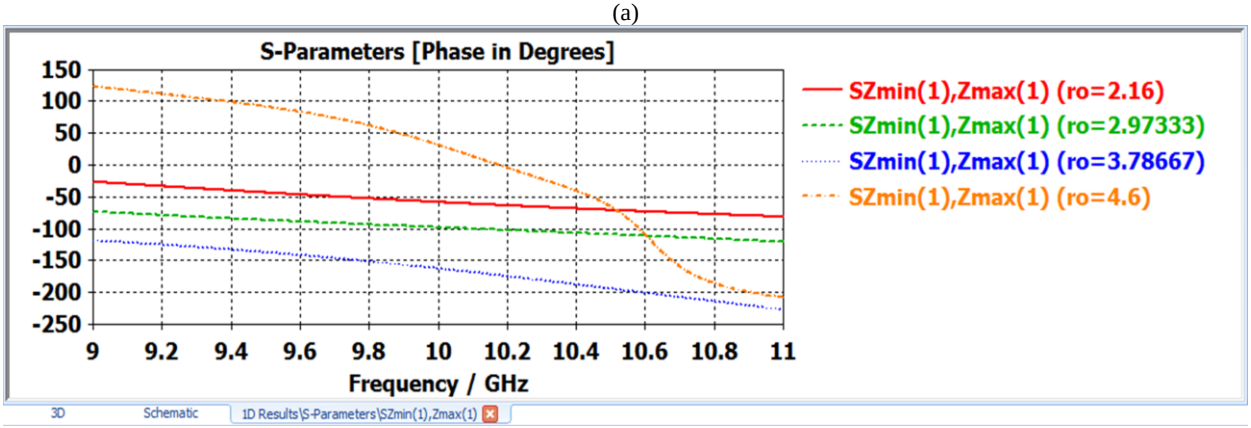

(b)

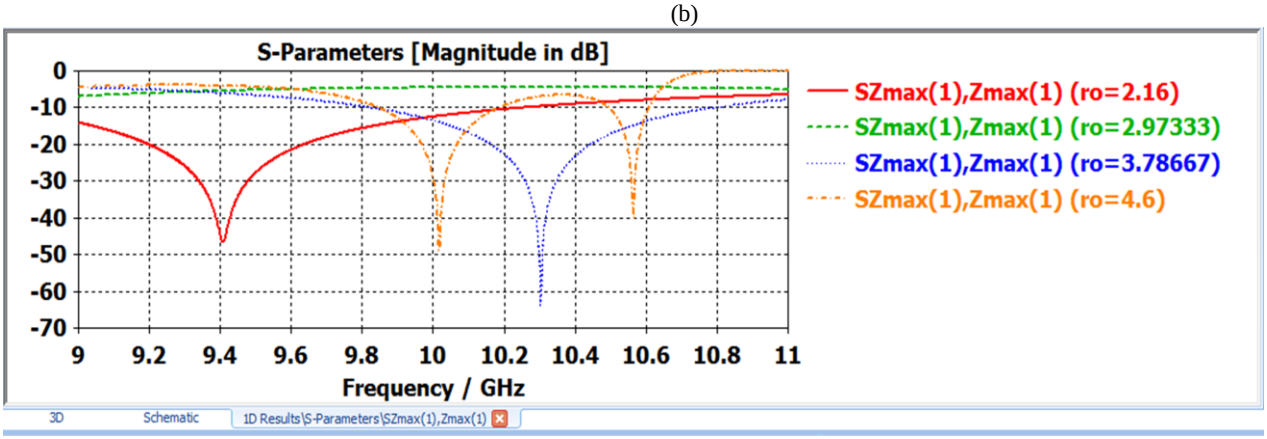

(c)

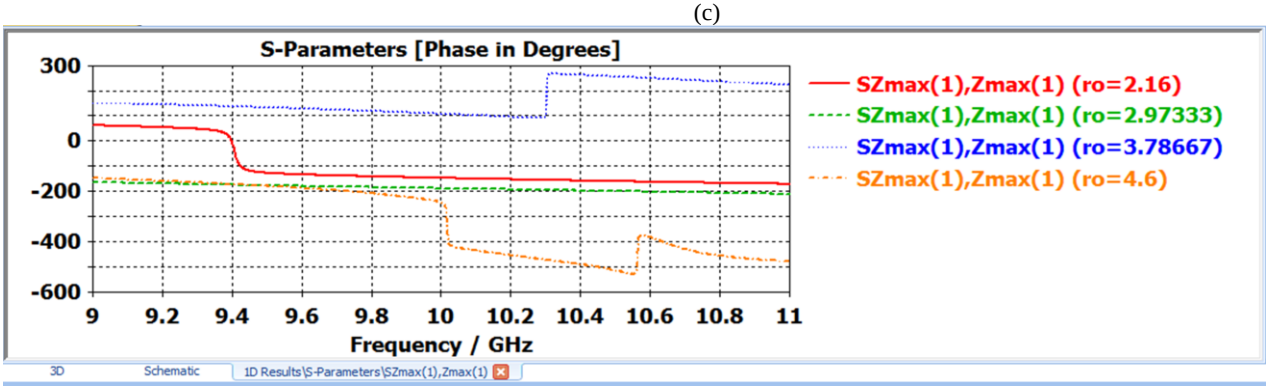

(d)

Figure 5. (a) Magnitude of S_{21} parameter of three layered dielectric (b) Phase of S_{21} parameter of three layered dielectric (c) Magnitude of S_{11} parameter of three layered dielectric (d) Phase of S_{11} parameter of three layered dielectric

III. DESIGN OF METASURFACE LENS

Researchers have developed an artificial thin surface lens that can reflect and focus electromagnetic waves which leads to the design of ultrathin low profile antennas. In visible spectrum these antennas work efficiently. This lens antenna can resolve nano scale features separated by very small distances in wavelengths. A plane wave or quasi-plane wave antenna is excited by using CST software, where patch antenna i.e. 30mm along the '–Z' direction at XY plane is placed away from metasurface. Here we have to analyze the gain, S-parameters and the 3-D simulated far field radiation pattern for F=30mm at 10 GHz, where F is the distance between patch antenna and phase gradient metasurface in a small scale range.

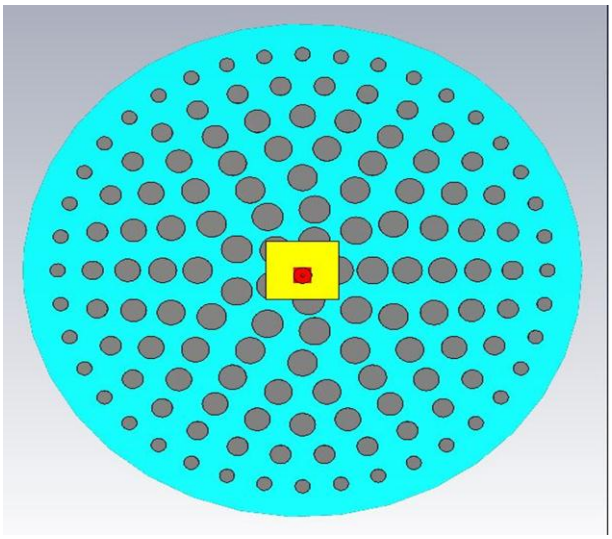

(a)

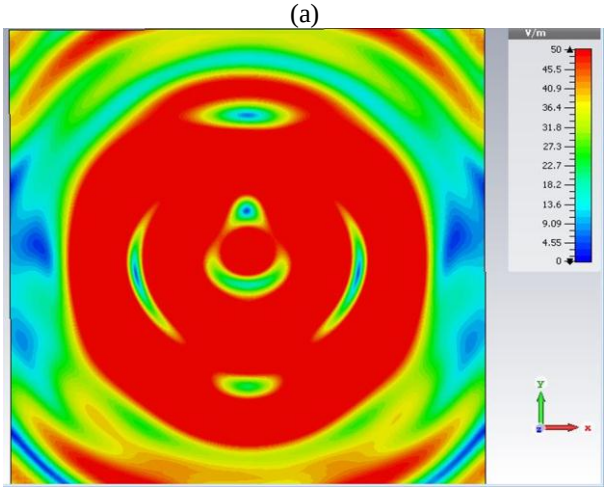

(b)

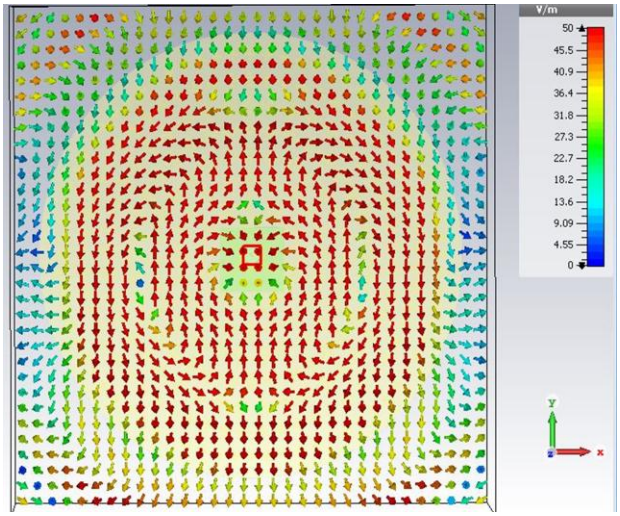

(c)

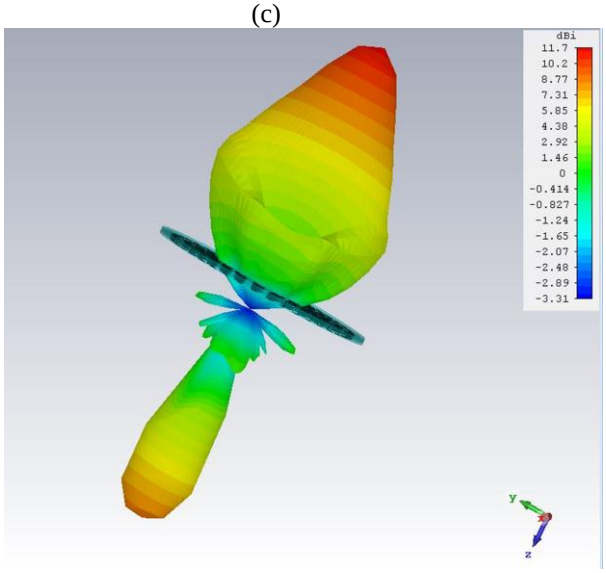

(d)

Figure 6. (a) Front view of unitcell element (b) Near field vector variation (c) Near electric field variation (d) Far field radiation pattern

In Fig.6 (a) the front view of unit cell device is shown, the phase gradient meta surface lens transforms the quasi sphere wave emitted by the patch antenna to plane wave as the theoretical prediction in both the planes which is shown in Fig. 6 (b, c) . Due to the high directivity of plane wave the beam width of the patch antenna will be decreased greatly and the gain will be enhanced remarkably. Fig.6 (b, c) shows the near field vector variation, near field electric field variation and absolute variation. The 3-D far field radiation pattern shown in Fig.6 (d), which gives a gain of 11.7 dBi but in case of normal microstrip antenna lens it is 7dBi. So a

gain enhancement of approximately 4.7 dBi is achieved which is shown in Y-Z plane.

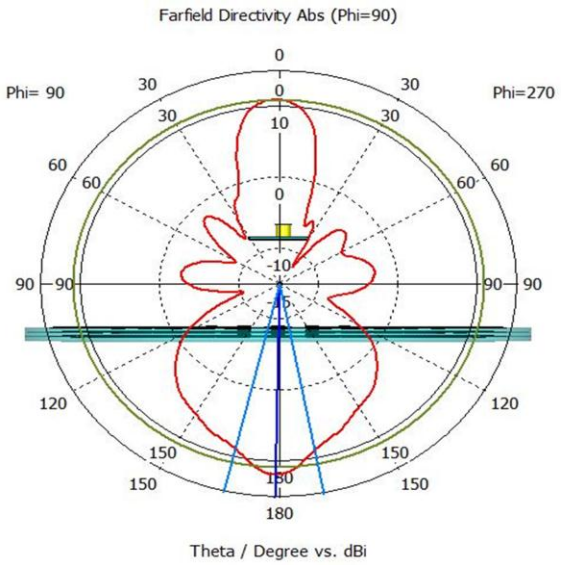

Figure 7. Polar plot of field radiation pattern of a metasurface lens antenna.

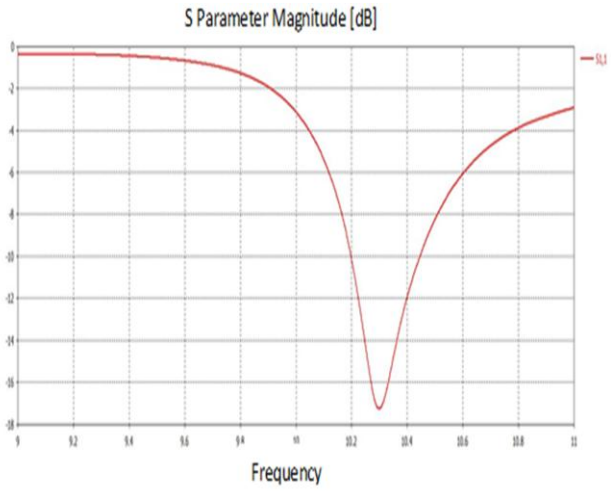

Figure 8. The S-parameter and return loss of a metasurface lens antenna for the field radiation pattern

The polar plot of the far field varies from the 0^0 to 360^0 which is shown in Fig. 7 which shows the distribution of power is maximum in 150^0 to 210^0. The return loss of the meta surface lens antenna is shown in Fig. 8 where the S-parameter magnitude in dB and frequency in GHz is shown. Approximately -17 db of power delay or return loss is observed at 10.3GHz frequency range.

IV. CODED METASURFACE ANTENNA DESIGN

A digital meta material is proposed where the artificial structures are explained by using two steps. Initially the coding meta materials that comprises of two types of unitcells with 0 and π phase response and named as 0 and 1 element. Then 0 and 1 is coded with controlled sequence (1-bit, 2-bits or 3-bits coding). In this paper the two bits coding is considered where four types of unitcells with different phase responses are presented. The phase $\varphi_n = n\pi/2$, where $n = 0,1,2,3$ and the phase responses $0, \pi/2, \pi, 3\pi/2, 2\pi$ are used for 00,01,10,11 elements.

A. Design of Coded Metasurface Antenna

Initially the elements are taken in sequences like 00,01,10,11 according to the phase distribution curve. Then the phase is quantized and divided in to eight discrete elements by observing the S_{21} phase diagram shown in Fig. 5 (b). A super cell containing 16 elements is distributed along X and Y axis in a 4×4 matrix. These are shown in Table 1 and Table 2. The four elements are distinguished by four radius as $r_1 = 2.16$ mm that is 00 element, $r_2 = 2.9$ mm that is 01 element, $r_3 = 3.7$ mm that is 10 element, $r_4 = 4.60$ mm that is 11 element.

Model 1

Model 1 shows a linear coded super cell with the sequence of elements as 00,01,10,11. Table 1 shows the 4×4 matrix of a linear coded super cell and Fig. 9 represents the front view of the 16×16 matrix with coded metasurface.

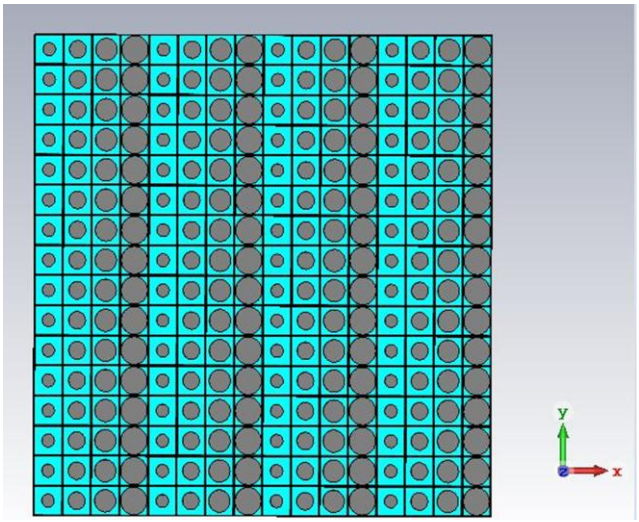

Figure 9: Front view of a coded 16X16 coded matrix of model 1

Table 1

00	**01**	**10**	**11**
00	**01**	**10**	**11**
00	**01**	**10**	**11**

00	**01**	**10**	**11**

Here a microstrip coaxial feed antenna at 10 GHz frequency is used, which is put away from the design at 1λ (λ=30mm) and excited by plane waves. Generally the wave move in plane or 0° but we get a $30^{\circ} to\ 40^{\circ}$ phase change, so it is possible to bend the beam or to steer the beam by using such kind of principle. In Fig.10 (a, b) the front view radiation pattern in X-Y plane and far field in X-Z plane are shown. This principle is also applicable for Model 2.

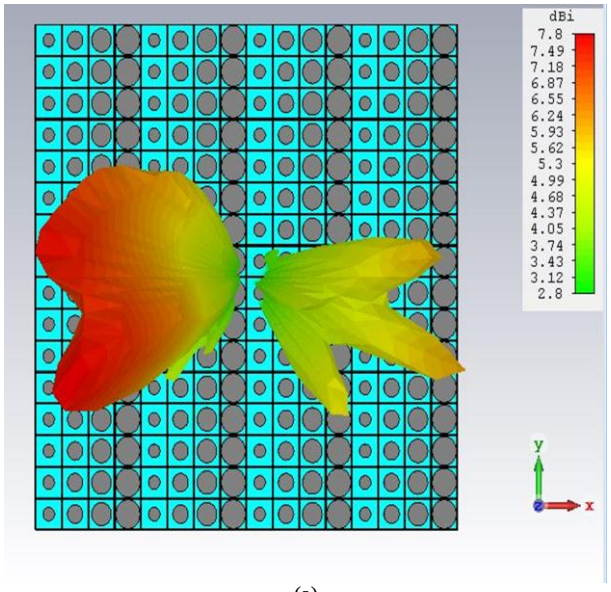

(a)

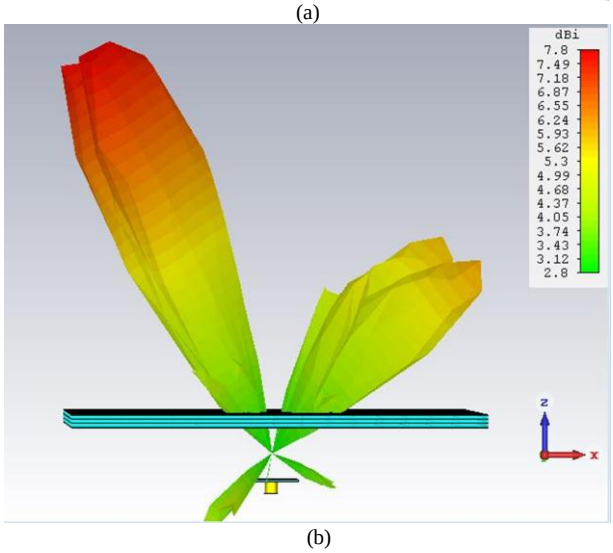

(b)

Figure 10: (a) Front view of radiation pattern (b) side view radiation pattern in X-Z plane

The linear distribution of electric field of model 1 is shown in Fig. 11. As the microstrip lens antenna is placed at the center, so the field distribution is more at the center.

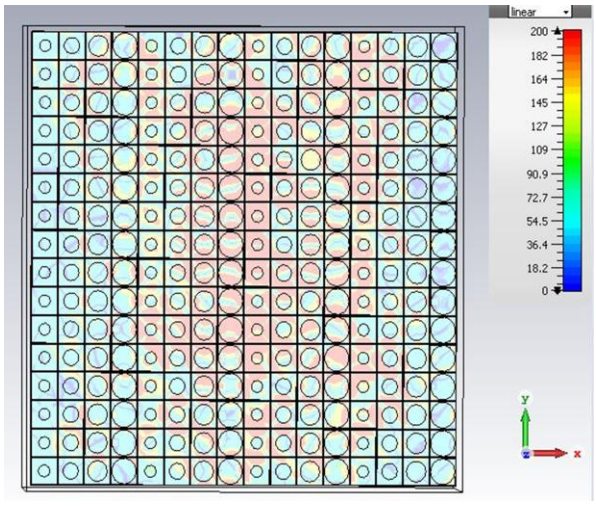

Figure 11. Linear distribution of electric field of model 1

Model 2

Model 2 shows the 180° phase shift of a super cell. In Table 2 an 4 × 4 anti phase of a super cell is presented and the front view of a 16 × 16 matrix coded metasurface is shown in Fig. 12. The sequences of the super cell elements are in the form of 10,11,00,01 accordingly.

Table 2

10	**00**	**10**	**00**
11	**01**	**11**	**01**
00	**10**	**00**	**10**
01	**11**	**01**	**11**

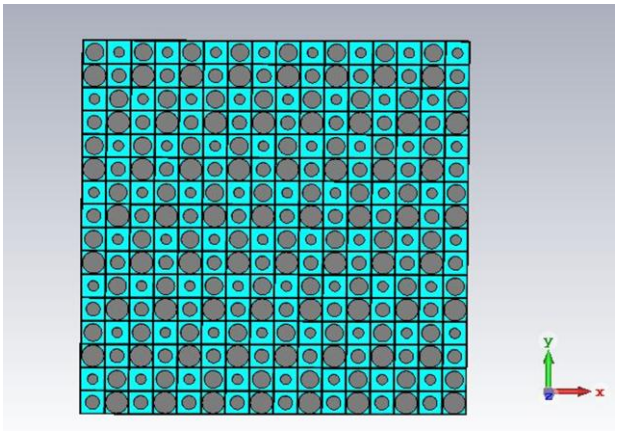

Figure 12: Front view of a coded 16X16 coded matrix of model 2

Fig.13 (a, b) shows the side view and the front view radiation pattern or the far filed radiation pattern of 180° phase change.

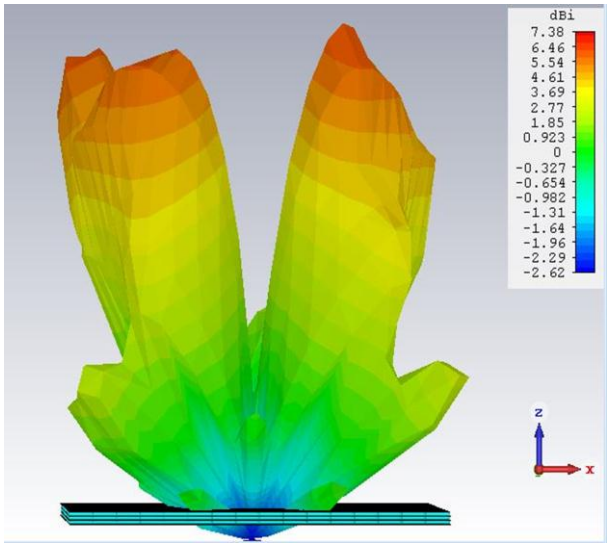

(a)

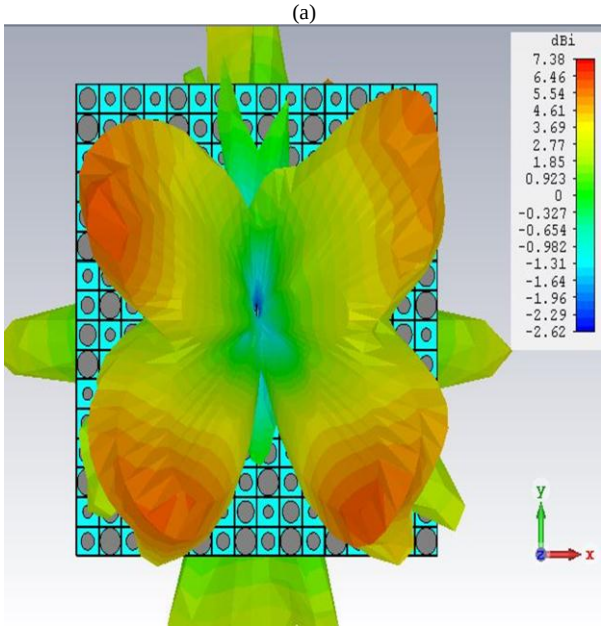

(b)

Figure 13. (a) Side view of radiation pattern in XZ plane (b) front view radiation pattern in XY plane

Two beams are formed due to the 180° phase shift in the side view of the metasurface in X-Z plane, four lobs formed and each lob is bending by 30° phase in X-Y plane. The electric field distribution of model 2 with supercell elements of 10,11,00,01 having 180° phase shift has given in Fig. 14.

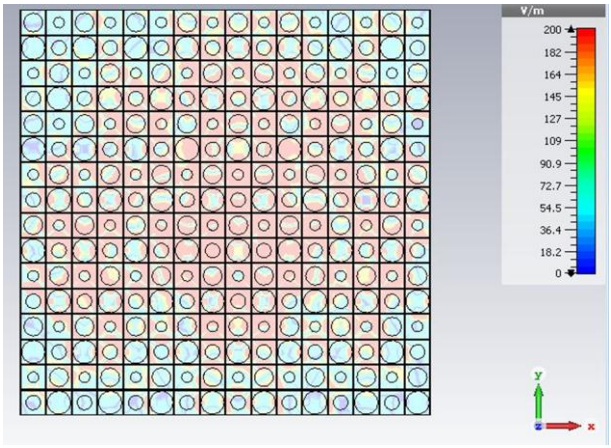

Figure 14. Linear distribution of electric field of model 2

B. Comparision between Microstrip and Lens Antenna

In this section a comparison of S_{11} parameter of a normal microstrip antenna and coded metasurface lens antenna is presented. It can be analyzed from Fig. 15 that approximately -12 dB return loss observed from normal microstrip antenna whereas -34 dB is observed in case of coded lens antenna. Thus microstrip lens antenna gives better performance as compared to normal microstrip antenna.

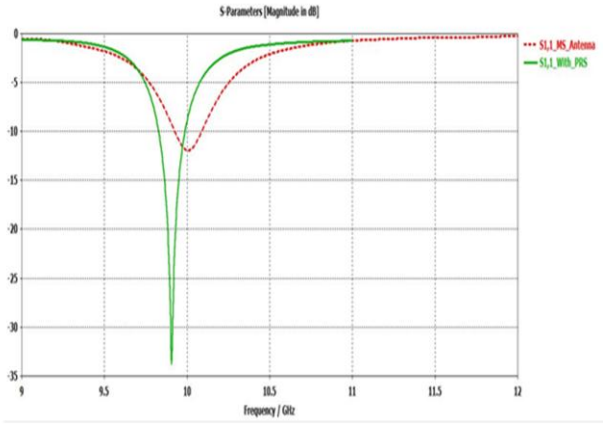

Figure 15. S_{11} Parameter comparison of normal microstrip antenna and coded PGMS microstrip antenna

V. CONCLUSION

The phase gradient metasurface with high gain transmitting lens antenna at X band frequency and two bits coded metasurface with four types of unitcell is simulated with the phase and amplitude response for X-band radar applications. An enhanced gain of 11.7 dBi is observed in case of microstrip lens antenna where as in case of normal microstrip

antenna it is 7 dB. Along with gain enhancement a power delay or return loss of - 17 dB has been found at 10.3 GHz frequency range. A comparison of S_{11} parameter between a normal microstrip antenna and coded metasurface lens antenna is analysed and -34 dB is observed.

REFERENCES

[1] H. Li, G. Wang, X. He-Xiu, T. Cai, "*X-band phase-gradient metasurface for high-gain lens antenna application*", IEEE Transactions on Antennas and Propagation, Vol. **63**, Issue.**11**, pp. **5144-5149,2015**.

[2] Y. Zhou, C. Xiang-yu, G. Jun G, "*RCS reduction for grazing incidence based on coding metasurface*", Electronics Letters, Vol. **53**, Issue. **20**, pp. **1381-1383, 2017.**

[3] X. Li, S. Xiao, B. Cai, H. Qiong, "*Flat metasurfaces to focus electromagnetic waves in reflection geometry*", Optics letters, Vol. **37**, Issue. **23**, pp. **4940-4942, 2012**.

[4] B. Rahmati, H. R. Hassani, "*Low-profile slot transmit array antenna*", IEEE Transactions on Antennas and Propagation, Vol. **63**, Issue.**1**, pp.**174-181, 2015.**

[5] Z. Yue-Jun, G. Jun, Z. Yu-Long, "*Metamaterial-based patch antenna with wideband RCS reduction and gain enhancement using improved loading method",* IET Microwaves, Antennas & Propagation, Vol. **11**, Issue. **9**, pp. **1183-1189, 2017**.

[6] S. Liu, C. Tie, X. Quan, "*Anisotropic coding metamaterials and their powerful manipulation of differently polarized terahertz waves*", Light: Science & Applications, Vol. **5**, pp. **16076, 2016**.

[7] N. Yu, G. Patrice, A. Kats, "*Light propagation with phase discontinuities: generalized laws of reflection and refraction*", *Science*, **6054**, pp. **333-337, 2011.**

[8] K. S. Beenamole, "*Microstrip Antenna Designs for Radar Applications*", DRDO Science Spectrum, pp. **84-86, 2009.**

[9] J. Shi, F. Xu, P. Eric, "*Coherent control of Snell's law at metasurfaces*", Optics express, Vol. **22**, Issue. **17**, pp. **21051-21060, 2014**.

[10] W. E. Liu, Z. N. Chen, X. Qing, J. Shi, F.H. Lin, "*Miniaturized Wideband Metasurface Antennas*," IEEE Transactions on Antennas and Propagation, Vol. **65**, Issue .**12**, pp.**7345-7349, 2017.**

[11] X. Liu, J. Gao, L. Xu, X. Cao, Y. Zhao, S. Li, S., "*A coding diffuse metasurface for RCS reduction*," IEEE Antennas and Wireless Propagation Letters, Vol.**16**, pp. **724-727, 2017.**

[12] C. L. Holloway, E. F. Kuester, J. A. Gordon, J. O' Hara, J. Booth, D. R. Smith, "*An overview of the theory and applications of metasurfaces: The two- dimensional equivalents of metamaterials*," IEEE Antennas and Propagation Magazine, Vol. **54**, Issue. **2**, pp. **10-35, 2012**.

[13] F. Y. Kuo, R. B. Hwang, "*High-isolation X-band marine radar antenna design*," IEEE Transactions on Antennas and Propagation, Vol. **62**, Issue**. 5**, pp. **2331-2337, 2014**.

[14] J. Li, D. Jiang, "*Low-complexity propagator based two dimensional angle estimation for coprime MIMO radar*," IEEE Access, Vol. **4**, Issue. **2,2018.**

